Supplemental Table 1. Forward (F) and Reverse (R) Primers for Real-Time PCR

Gene Name	Gene ID	Sequence
IL-4	16189	F: GGTCTCAACCCCCAGCTAGT R: CCGATGATCTCTCTCAAGTGAT
IL-10	16153	F: GATGCCCCAGGCAGAGAA R: CACCCAGGGAATTCAAATGC
TNFα	21926	F: CAGCCGATGGGTTGTACCTT R: GGCAGCCTTGTCCCTTGA
CCL2	20296	F: GTCTGTGCTGACCCCAAGAAG R: TGGTTCCGATCCAGGTTTTTA
CCL7	20306	F: CCACATGCTGCTATGTCAAGA R: ACACCGACTACTGGTGATCCT
CCL12	20293	F: ATTTCCACACTTCTATGCCTCCT R: ATCCAGTATGGTCCTGAAGATCA
ANP	230899	F: GCTTCCAGGCCATATTGGAG R: GGGGGCATGACCTCATCTT
BNP	18158	F: AAGAGAAAAGTCGGAGGAAATGG R: TTTGTGAGGCCTTGGTCCTT
ICAM	15894	F: GTGATGCTCAGGTATCCATCCA R: CACAGTTCTCAAAGCACAGCG
VCAM	22329	F: GCCCACTAAACGCGAAGGT R: ACTGGGTAAATGTCTGGAGCC
TGFβ	21803	F: CTCCCGTGGCTTCTAGTGC R: GCCTTAGTTTGGACAGGATCTG
TGFβR1	21812	F: TCTGCATTGCACTTATGCTGA R: AAAGGGCGATCTAGTGATGGA
TGFβR2	21813	F: TTGGATTGCCAGTGCTAACCC R: AACAAGCCACAGTAACATGACA
Collagen I	12842	F: CTTCACCTACAGCACCCTT R: TGACTGTCTTGCCCCAAAGT
Collagen III	12825	F: TTCTGCCACCCCGAACTC R: TTGCAGCCTTGGTTAGGATCA
Collagen IV	12828	F: AGCTCTCGAACCCTATATTA R: TGAACAGCTATCGCCATTG
Fibronectin	14268	F: AGGCAGAAAACAGGTCTCGATT R: TGAATGAGTTGGCGGTGATATC
Vimentin	22352	F: GAGAGAGGAAGCCGAAAGCA R: GCCAGAGAAGCATTGTCAACAT
GAPDH	14433	F: CATGGCCTTCCGTGTTCCTA R: GCGGCACGTCAGATCCA
β-Actin	11461	F: CGATGCCCTGAGGCTCTTT R: TGGATGCCACAGGATTCCA

SUPPLEMENTAL FIGURE LEGENDS

Supplemental Figure1. Identification of cardiac macrophages in naïve mouse hearts by flow cytometry. ***A)*** Depiction of gating strategy used to identify $CD45^{+}F4/80^{+}MerTK^{+}$ cardiac macrophages using flow cytometry, and differentiation of $CCR2^{-}$ resident and $CCR2^{+}$ infiltrating macrophage sub-populations in naïve mice. ***B)*** Corresponding quantitation of $CD45^{+}$ leukocytes, $F4/80^{+}MerTK^{+}$ macrophages, and $CCR2^{+}$ and $CCR2^{-}$ macrophage subsets from mouse hearts.

Supplemental Figure 2. Identification of circulating monocytes by flow cytometry. Illustration of peripheral blood leukocyte gating strategy to identify $Ly6C^{hi}CCR2^{+}$ and $Ly6C^{low}$ monocytes. Monocytes were pre-gated on $CD45^{+}CD11b^{+}Ly6G^{-}$ cells.

Supplemental Figure 3. CCR2 antagonism with RS-504393 during acute pressure overload blunts early compensatory left ventricular (LV) hypertrophy. LV end-diastolic volume (EDV), end-systolic volume (ESV), ejection fraction (EF), end-diastolic interventricular septum thickness (IVSd), and end-diastolic LV posterior wall thickness (LVPWd) (***A***), and aortic gradient (***B***) as measured by echocardiography and Doppler in mice treated with CCR2 antagonist or vehicle 6 d after transverse aortic constriction (TAC) or sham operation. ***C***) Heart weight (HW) to tibia length (TL) ratio 1 w after TAC or sham operation. N=11-14 per group for panels A-C. ***D***), LV gene expression of the hypertrophic markers atrial and B-type natriuretic peptide (ANP and BNP) 1 w post-TAC or sham operation. (n=5-6 per group). ***E***) Representative cardiac wheat germ agglutinin stains and cardiomyocyte area quantitation for the same experimental groups (n=4-6 per group). Scale bar 25μm. *p<0.01, **p<0.01, ***p<0.001; ****p<0.0001. Statistical comparisons for ANP gene expression and cardiomyocyte area performed after logarithmic data transformation as described in text.

Supplemental Figure 4. Cardiac macrophage quantitation in mice treated with MC21 or IgG 4 w after TAC or sham-operation. The flow cytometry gating strategy outlined in Figure 1 was used to identify monocyte-derived infiltrating $CCR2^{+}$ macrophages (*Left*) and $CCR2^{-}$ resident macrophages (*Right*), pre-gated on $F4/80^{+}MerTK^{+}CD64^{+}$ cells. Statistical comparisons were performed using individual unpaired t-test or Mann-Whitney test (as appropriate) between the four specific experimental groups, with Bonferroni post-hoc correction as detailed in the text. A $p < 0.0125$ was used for statistical significance.

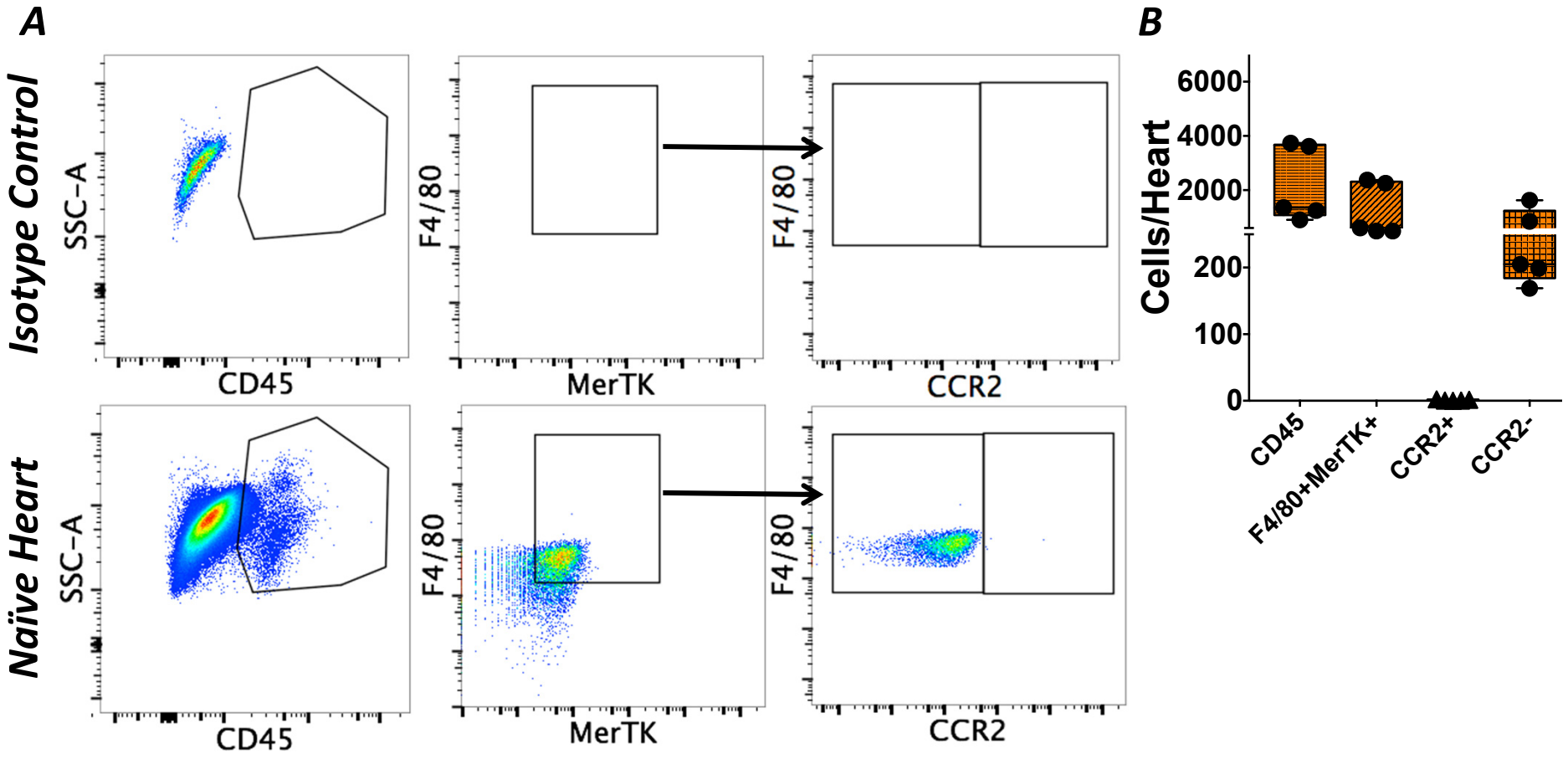

Supplemental Figure 1

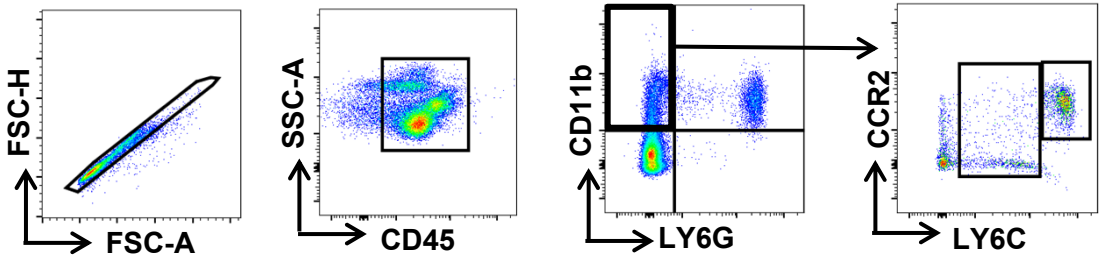

Supplemental Figure 2

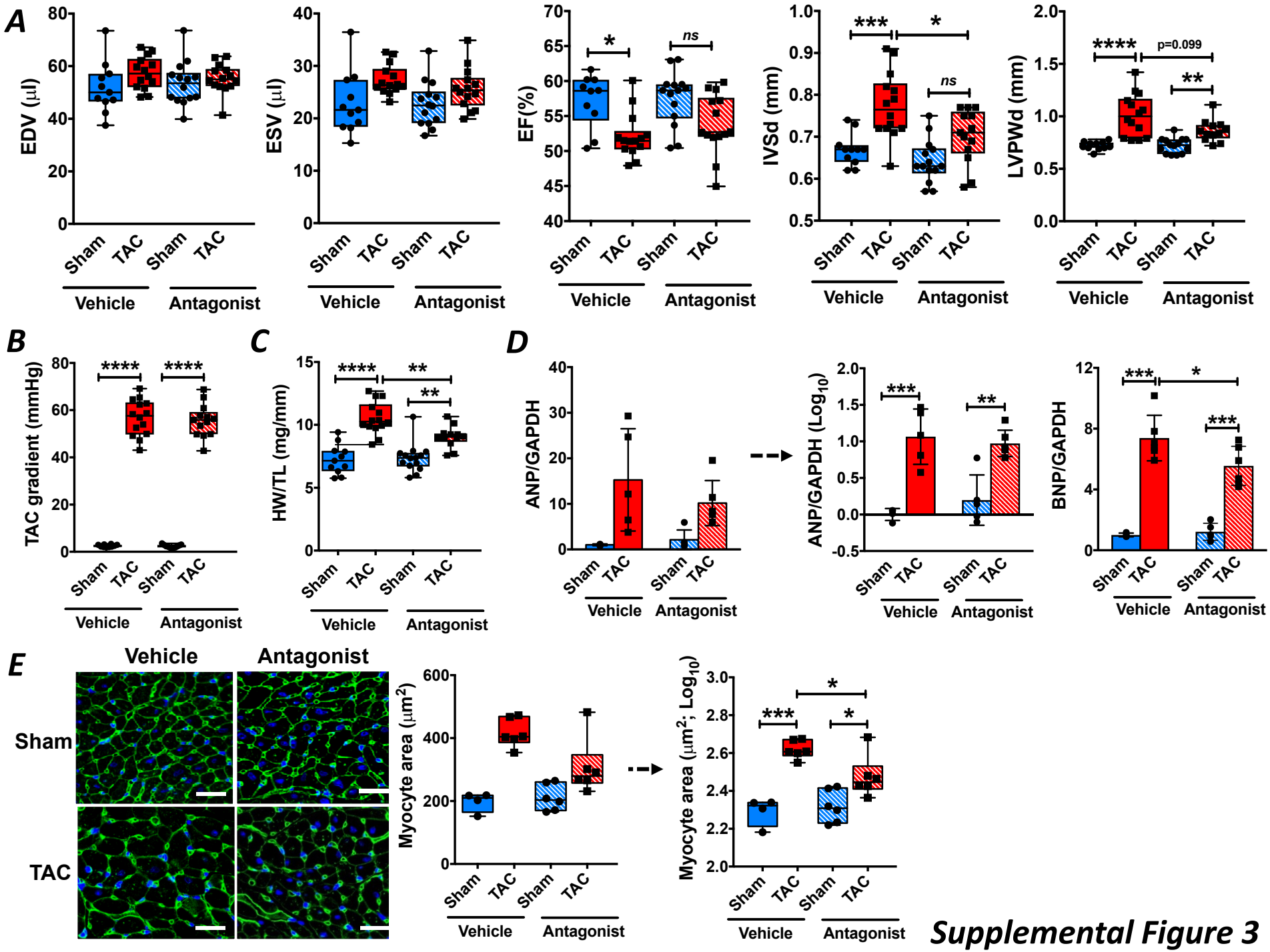

Supplemental Figure 3

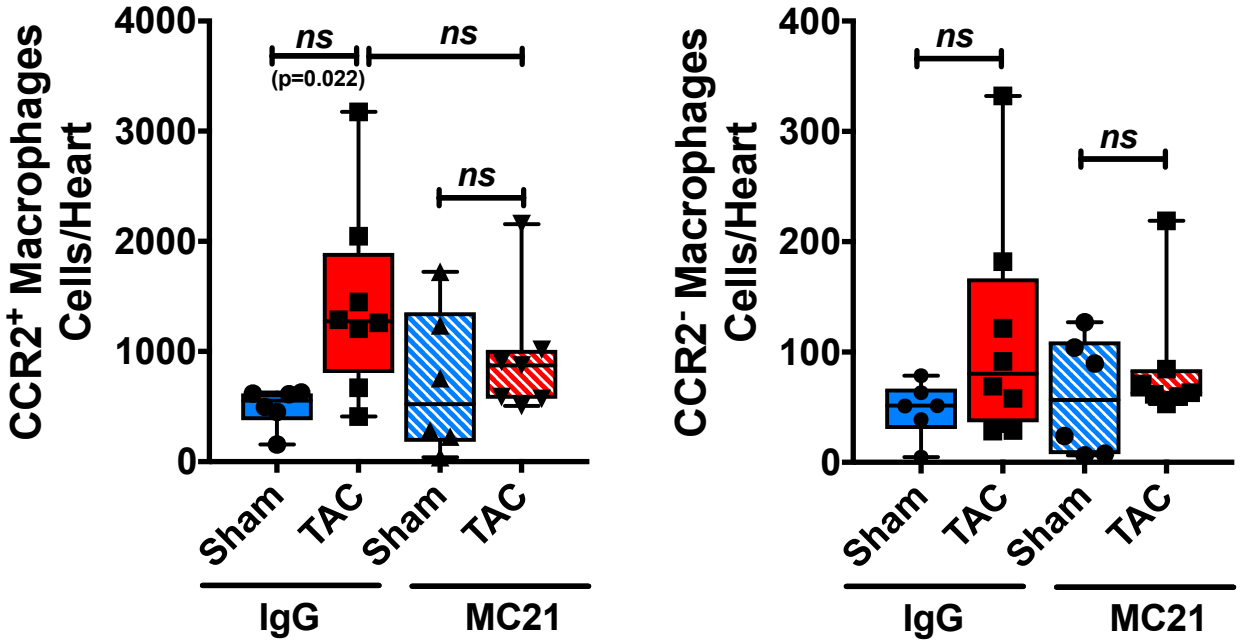

Supplemental Figure 4